JITK (JURNAL ILMU PENGETAHUAN DAN TEKNOLOGI KOMPUTER)

VOL. 11. NO. 3 FEBRUARI 2026
P-ISSN: 2685-8223 | E-ISSN: 2527-4864
DOI: 10.33480/jitk.v11i3.7131

OPTIMIZING VGG-16 CONVOLUTIONAL NEURAL NETWORK FOR PAP SMEAR IMAGE CLASSIFICATION IN CERVICAL CANCER DETECTION

Odi Nurdiawan[1]; Heliyanti Susana[2*]; Ade Rizki rinaldi[3]; Ahmad Asyraful Hijrah[3]; Indah Diniarti[4]

Informatics Management[1]
Informatics Engineering[2]
Software Engineering[3]
Information Systems[4]
STMIK IKMI Cirebon, Cirebon, Indonesia[1,2,3,4]
http://ikmi.ac.id/
odinurdiawan2020@gmail.com, heliyanti.ikmi@gmail.com*, rizki.ikmi@gmail.com,
ahmad.ikmi@gmail.com, indah.ikmi@gmail.com.

(*) Corresponding Author
(Responsible for the Quality of Paper Content)

Abstract—*Early detection of cervical cancer through Pap smear image analysis plays a crucial role in reducing mortality rates associated with this disease. This study aims to optimize the VGG16 architecture to improve the classification accuracy of Pap smear images. The proposed method employs transfer learning with pre-trained ImageNet weights, customization of fully connected layers, and data augmentation techniques to enhance the diversity of training images. Experimental results demonstrate a significant improvement in training accuracy, reaching 98.50%, while validation accuracy remained stable at 88.24%, indicating potential overfitting. Performance testing on unseen data yielded an accuracy of 80%, with high precision for the negative class but low recall for the positive class, suggesting a bias toward the majority class. These findings highlight the need for additional strategies, such as data balancing and hybrid method integration, to improve sensitivity to positive cases. This research contributes to the development of adaptive deep learning-based classification models that support clinical decision-making in cervical cancer screening and opens opportunities for further research on model optimization and dataset expansion.*

Keywords *: Cervical Cancer, Image Classification, Pap Smear, Transfer Learning, VGG16*

Intisari—*Deteksi dini kanker serviks melalui analisis citra Pap Smear memiliki peran penting dalam menekan angka kematian akibat penyakit ini. Penelitian ini bertujuan mengoptimalkan arsitektur VGG16 untuk meningkatkan akurasi klasifikasi citra Pap Smear. Metode yang digunakan meliputi transfer learning dengan bobot pra-latih dari ImageNet, penyesuaian lapisan fully connected, dan teknik augmentasi data untuk meningkatkan keragaman citra latih. Hasil pelatihan menunjukkan peningkatan akurasi signifikan pada data latih hingga 98,50%, namun akurasi validasi cenderung stabil di angka 88,24%, yang mengindikasikan potensi overfitting. Uji performa pada data baru menghasilkan akurasi 80%, dengan precision tinggi pada kelas negatif tetapi recall rendah pada kelas positif, menandakan bias terhadap kelas mayoritas. Temuan ini memperkuat perlunya strategi tambahan seperti penyeimbangan data dan integrasi metode hibrid untuk meningkatkan sensitivitas terhadap kasus positif. Penelitian ini memberikan kontribusi penting dalam pengembangan model klasifikasi berbasis deep learning yang adaptif untuk mendukung sistem pendukung keputusan klinis pada skrining kanker serviks, serta membuka peluang penelitian lanjutan pada optimasi model dan perluasan data*.

Kata Kunci : *Kanker Serviks, Klasifikasi Citra, Pap Smear, Pembelajaran Transfer, VGG16.*

INTRODUCTION

Cancer remains one of the leading causes of death worldwide, with high morbidity and mortality rates, including in Indonesia[1], [2]. Early detection of cancer plays a crucial role in increasing the success rate of treatment and reducing mortality rates. In this context, advancements in Artificial Intelligence (AI), particularly deep learning, have led to significant progress in medical image analysis[3], [4], [5]. Among the most widely used approaches is the Convolutional Neural Network (CNN), with the VGG16 architecture being one of the most frequently adopted models due to its proven ability to effectively extract complex features from medical imaging data [6], [7],[8].

The use of VGG16 in cancer diagnosis has been reported for various cancer types, including lung cancer, breast cancer, and cervical cancer[8], [9], [10]. Developed by the Visual Geometry Group at the University of Oxford, VGG16 comprises 16 layers with an architectural depth that facilitates high-level feature extraction. In studies by Klangbunrueang . (2025) and Lakide (2025), VGG16 demonstrated its effectiveness in classifying lung cancer CT scan images into normal, benign, and malignant categories, thereby assisting radiologists in making more accurate diagnostic decisions[11], [12].

Nonetheless, challenges remain in interpreting complex medical images, such as overlapping features between benign and malignant lesions, limited training data, and variability in image quality. This is where transfer learning becomes particularly valuable. By leveraging pre-trained VGG16 weights, training can be more efficient, and accuracy can be improved, as shown by Lakide (2025) for lung cancer detection and Hameed et al. (2020) for breast cancer histopathological classification[12], [13], [14], [15].

In the context of cervical cancer, VGG16 has also been applied to classify histopathology and colposcopy images with promising results [16], [17]. The use of techniques such as data augmentation, early stopping, and fine-tuning has been shown to enhance model performance. Valdés & Interian [18] demonstrated that integrating CNNs with optimization strategies can effectively predict rectal toxicity in cervical cancer patients, contributing to the personalization of radiotherapy treatment. Additionally, Yadav et al. (2022) emphasized the potential of CNNs, including VGG16, in detecting precancerous lesions through histopathological image analysis with high accuracy[19], [20].

Recent research focusing specifically on Pap Smear classification further demonstrates the potential of CNNs. Maurya et al. (2023) proposed *VisionCervix*, integrating CNN and Vision Transformer, achieving 97.65 % accuracy on Pap-Smear images [18]. Mishra et al. (2023) developed a *Hybrid Pooling-Based CNN* to improve morphological-feature representation, reducing false-negative detection [25]. Attallah (2023) introduced *CerCan·Net*, combining lightweight CNNs through multi-layer feature ensembles, yielding more stable recall on minority (positive) classes [23]. Yang et al. (2025) proposed a *Pyramid Convolutional Mixer* architecture to enhance feature learning efficiency in Pap-Smear image classification [22].

However, misclassification issues caused by morphological similarities between benign lesions, such as chronic cervicitis, and neoplastic tissues remain a challenge (Huang et al., 2022). This underscores the importance of developing more sophisticated methods, including multimodal data integration and the application of attention mechanisms, to enhance diagnostic reliability[21], [22], [23], [24].

Recent literature from the Scopus database also shows rapid advancements in cervical cancer detection methods using CNNs and hybrid variants. For example, Vision Cervix Maurya, 2023, which integrates Vision Transformer with CNN, achieved an accuracy of 97.65% [18]. Similarly, a deep feature selection approach based on Opposition-based Harmony Search Das 2023 improved classification performance [25]. Other notable models include CNN-LSVM Wu, 2023 and the integration of 3D CNN with Vision Transformer K. & Sivakumar, 2024, which excel in processing spatiotemporal data and high-level features. These findings indicate that integrating VGG16 as a backbone in hybrid systems can be a promising strategy [26], [27].

Considering these various approaches, a research gap can be identified in the application of VGG16 for cervical cancer detection, particularly in addressing the challenges of limited data, complex tissue morphology, and the need for interpretable results. This study aims to develop and optimize a VGG16-based model for cervical cancer classification by employing transfer learning, data augmentation, and the integration of attention mechanisms. The novelty of this research lies in the optimization of VGG16 architecture tailored to the classification of cervical cancer images, as well as evaluating its performance on multi-source data to improve the accuracy and reliability of early detection.

Accredited Rank 2 (Sinta 2) based on the Decree of the Dirjen Penguatan RisBang Kemenristekdikti No.225/E/KPT/2022, December 07, 2022. Published by LPPM Universitas Nusa Mandiri

VOL. 11. NO. 3 FEBRUARI 2026
P-ISSN: 2685-8223 | E-ISSN: 2527-4864
DOI: 10.33480/jitk.v11i3.7131

MATERIALS AND METHODS

The research workflow is designed to systematically describe each stage of the study, from the initial problem identification to the final evaluation of model performance. The methodology is divided into three main stages, as illustrated in Figure 1.

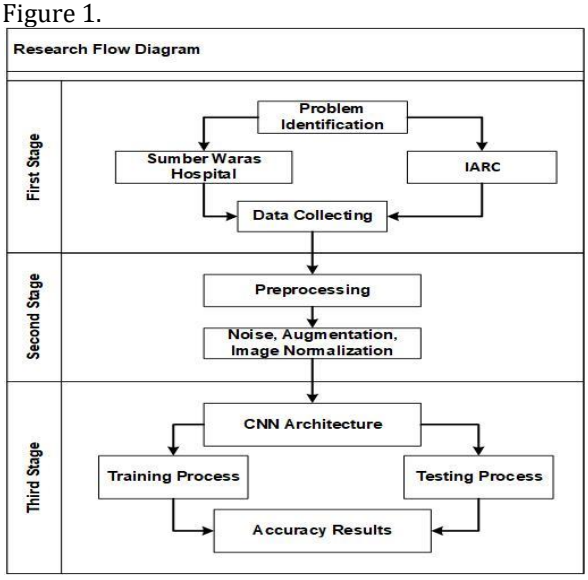

Source : (Research Results, 2025)
Figure 1. Research Workflow of the Proposed VGG16-Based Cervical Cancer Detection System Diagram

1. First Stage : Problem Identification and Data Collection

The initial stage involved identifying the research problem. The problem was defined based on two primary sources: Sumber Waras Hospital and the International Agency for Research on Cancer (IARC). Following problem identification, a data collection process was conducted, in which Pap smear images were obtained from both sources. These data served as the foundation for subsequent stages of the research.

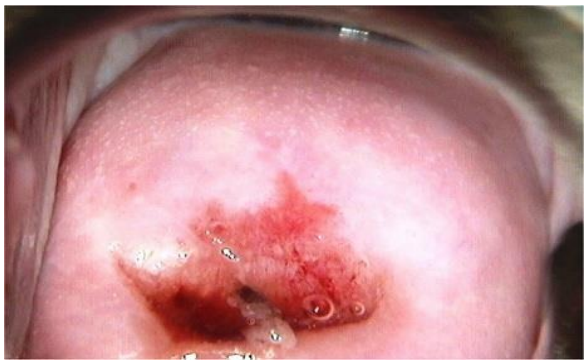

Source : (Research Results, 2025)
Figure 2. Pap Smear

Figure 2 illustrates a Pap smear image showing an irregular red lesion in the cervical area. This highlights the importance of early detection as a key factor in reducing cervical cancer mortality rates.

2. Second Stage : Data Preprocessing

The preprocessing stage is a crucial step carried out after data acquisition to ensure that the images are in optimal condition for model training. The objective of preprocessing is to enhance data quality so that the model can learn effectively. In this study, preprocessing comprised three main processes:

1. Noise Removal The removal of unwanted noise or distortion in the images that could negatively impact classification accuracy.
2. Data Augmentation Techniques used to increase the diversity of the training data through image transformations, such as rotation, flipping, and scaling, to improve the model's robustness against variations in data.
3. Image Normalization Adjusting the pixel value scale to a consistent range, ensuring uniform input data that facilitates efficient model learning.

Through these preprocessing steps, the quality and diversity of the dataset were improved, thereby increasing the likelihood of achieving high classification accuracy.

3. Third Stage : Model Development, Training, and Testing

In the final stage, the preprocessed data were fed into the VGG16 Convolutional Neural Network (CNN) architecture for both training and testing. Training Process The model was trained using the training dataset to learn distinctive patterns, features, and characteristics from the Pap smear images. This involved adjusting model parameters to minimize classification errors. Testing Process The trained model was then evaluated using an independent test dataset that was not used during training. This process measured the model's generalization ability and provided an objective assessment of its classification performance. The resulting accuracy score served as the primary indicator of the model's performance, forming the basis for evaluating the effectiveness of the proposed method.

RESULTS AND DISCUSSION

Developing a robust image classification system requires a neural network architecture

capable of optimally extracting features from visual data. One of the most effective architectures for this task is VGG16, introduced by the Visual Geometry Group (VGG) at the University of Oxford. VGG16 leverages network depth through a hierarchical arrangement of convolutional layers, consistently applying small 3×33×3 kernels to capture spatial details at multiple representation levels.

Table 1. Model architecture of the VGG16

No	Layer (Type)	Output Shape	Parameters
1	input_layer (InputLayer)	(None, 224, 224, 3)	0
2	block1_conv1 (Conv2D)	(None, 224, 224, 64)	1.792
3	block1_conv2 (Conv2D)	(None, 224, 224, 64)	36.928
4	block1_pool (MaxPooling2D)	(None, 112, 112, 64)	0
5	block2_conv1 (Conv2D)	(None, 112, 112, 128)	73.856
6	block2_conv2 (Conv2D)	(None, 112, 112, 128)	147.584
7	block2_pool (MaxPooling2D)	(None, 56, 56, 128)	0
8	block3_conv1 (Conv2D)	(None, 56, 56, 256)	295.168
9	block3_conv2 (Conv2D)	(None, 56, 56, 256)	590.080
10	block3_conv3 (Conv2D)	(None, 56, 56, 256)	590.080
11	block3_pool (MaxPooling2D)	(None, 28, 28, 256)	0
12	block4_conv1 (Conv2D)	(None, 28, 28, 512)	1.180.160
13	block4_conv2 (Conv2D)	(None, 28, 28, 512)	2.359.808
14	block4_conv3 (Conv2D)	(None, 28, 28, 512)	2.359.808
15	block4_pool (MaxPooling2D)	(None, 14, 14, 512)	0
16	block5_conv1 (Conv2D)	(None, 14, 14, 512)	2.359.808
17	block5_conv2 (Conv2D)	(None, 14, 14, 512)	2.359.808
18	block5_conv3 (Conv2D)	(None, 14, 14, 512)	2.359.808
19	block5_pool (MaxPooling2D)	(None, 7, 7, 512)	0
20	flatten (Flatten)	(None, 25088)	0
21	dense (Dense)	(None, 128)	3.211.392
22	dropout (Dropout)	(None, 128)	0
23	dense_1 (Dense)	(None, 2)	258

Source : (Research Results, 2025)

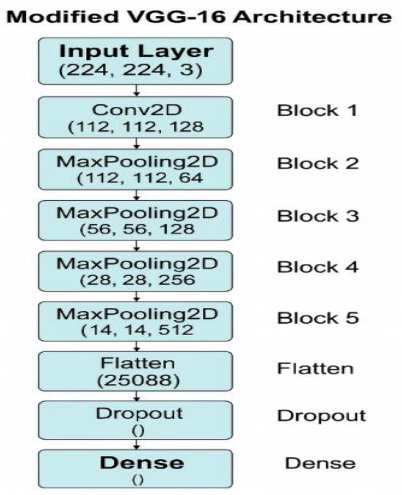

Source : (Research Results, 2025)

Figure 3. Layer Hierarchy Visualization on Models

Figure 3 and Table 1 presents the architecture of the VGG16 Convolutional Neural Network designed for digital image processing. The network receives an RGB image input of 224×224224 \times 224224×224 pixels via the input layer, which does not contain trainable parameters and serves solely as the entry point for image data. The VGG16 architecture is composed of five convolutional blocks, each followed by a max-pooling layer to reduce spatial dimensions while retaining essential image features:

1. Block 1: Two convolutional layers with 64 filters (3×33 \times 33×3) followed by max pooling, reducing the dimension to 112×112×64112 \times 112 \times 64112×112×64.
2. Block 2: Two convolutional layers with 128 filters (3×33 \times 33×3) followed by max pooling, producing 56×56×12856 \times 56 \times 12856×56×128.
3. Block 3: Three convolutional layers with 256 filters, ending with pooling to 28×28×25628 \times 28 \times 25628×28×256.
4. Block 4 & Block 5: Each contains three convolutional layers with 512 filters, extracting high-level and complex features, with pooling reducing dimensions to 7×7×5127 \times 7 \times 5127×7×512.

The output from the final pooling layer is flattened into a one-dimensional vector of 25,088 elements, which feeds into the fully connected layers:

1. Two dense layers of 4,096 units each with ReLU activation.
2. Dropout layers applied for regularization to reduce overfitting.

VOL. 11. NO. 3 FEBRUARI 2026
P-ISSN: 2685-8223 | E-ISSN: 2527-4864
DOI: 10.33480/jitk.v11i3.7131

3. An output layer using softmax activation with the number of units equal to the target classes.

This architecture comprises approximately 23.7 million parameters, of which 3.12 million are trainable, and 17.84 million are non-trainable pre-trained weights from ImageNet. This design enables efficient transfer learning, in which pre-trained weights remain fixed while fully connected layers are fine-tuned for the Pap smear classification task.

Model Training Performance

The VGG16 model was trained using transfer learning, where pre-trained weights for feature extraction were retained, and the customized fully connected layers were trained on the Pap smear dataset. Training parameters included an adaptively tuned learning rate, an optimal batch size for stable weight updates, and an appropriate number of epochs to ensure convergence. Preprocessing steps—such as resizing, pixel normalization, and data augmentation (rotation, flipping, zooming)—were applied to enhance dataset diversity and reduce overfitting risks.

Table 2. Presents training results:

Epoch	Accuracy	Loss	Val Accuracy	Val Loss
1	0,8121	0,5716	0,8824	0,3989
2	0,8518	0,4026	0,8824	0,3494
3	0,9037	0,2672	0,8824	0,3727
4	0,8898	0,239	0,8824	0,3304
5	0,9395	0,1677	0,8824	0,3353
6	0,9695	0,1314	0,8824	0,3238
7	0,9767	0,0953	0,8824	0,3122
8	0,969	0,091	0,8824	0,2979
9	0,9802	0,1013	0,8824	0,3373
10	0,985	0,0568	0,8824	0,3154

Source : (Research Results, 2025)

From the first epoch, the model achieved a training accuracy of 81.21% with a loss of 0.5716, while validation accuracy was already relatively high at 88.24% with a validation loss of 0.3989. This suggests that from the early stages of training, the model could capture key patterns in the data, likely due to the benefit of pre-trained weights. Between epochs two and three, training accuracy improved significantly from 85.18% to 90.37%, accompanied by a consistent reduction in loss. However, validation accuracy remained stable at 88.24%, indicating that the model reached convergence on the validation set early in the training process.

During epochs four to six, training accuracy continued to increase, reaching 96.95% with a notable drop in loss from 0.2390 to 0.1314. Despite this, validation accuracy did not improve and remained fixed at 88.24%, signaling the onset of overfitting, where further training improved performance on the training set but not on the validation set. By epochs seven to ten, training accuracy peaked at 98.50% with a very low loss of 0.0568. Validation accuracy still showed no improvement, staying constant at 88.24%, while validation loss fluctuated slightly within a narrow range (0.2979 – 0.3373). This indicates that although the model learned the training set well, limited diversity in the validation set constrained further improvements.

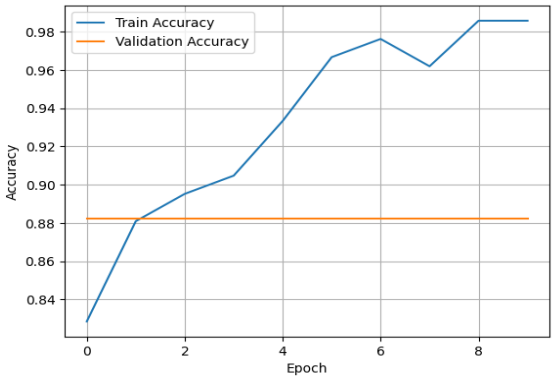

Source : (Research Results, 2025)
Figure 4. Epoch Graph

The training accuracy curve (blue line) shows a steep increase from around 81% in the first epoch to nearly 98% by the ninth epoch, indicating progressive learning of patterns and features from the training set. However, the validation accuracy curve (orange line) remained almost flat around 88% from the beginning to the end of training. This lack of improvement reflects early convergence and suggests that the model's ability to generalize to unseen data did not improve after the first epoch — a sign of potential overfitting.

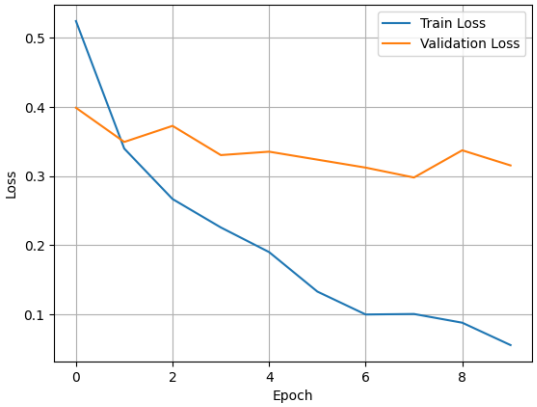

Source : (Research Results, 2025)
Figure 5. Loss Graph

The training loss curve (blue line) demonstrates a steady decrease from 0.57 in the

first epoch to about 0.05 in the final epoch, showing that the model increasingly minimized errors on the training set. In contrast, the validation loss curve (orange line) remained relatively stable between 0.30 and 0.40, with minor fluctuations. This lack of a significant downward trend in validation loss reinforces the earlier observation that the model's generalization capability did not improve notably after the early epochs.

Model Evaluation and Testing

After completing the training and validation phases, the model was further evaluated using a test dataset that had not been used during the training process. This step aimed to assess the model's generalization ability and provide an unbiased measure of its classification performance on unseen data.

Table 3. Summarizes the testing results for individual images:

File Name	Prediction	Percentage (%)
File Test_Negative_7.jpg	Negative	62,6
File Test_Negative_1.jpg	Negative	62,9
File Test_Positive_1.jpg	Negative	95,6
File Test_Positive_4.jpg	Negative	80,0
File Test_Negative_12.jpg	Negative	74,6
File Test_Negative_8.jpg	Negative	62,6
File Test_Positive_10.jpg	Negative	86,5
File Test_Negative_22.jpg	Negative	76,1
File Test_Negative_6.jpg	Negative	70,5
File Test_Negative_28.jpg	Negative	75,0
File Test_Positive_2.jpg	Positive	65,0

Source : (Research Results, 2025)

Overall Accuracy and Class-wise Performance

Classification Report:

	precision	recall	f1-score	support
negatif	0.79	1.00	0.88	30
positif	1.00	0.20	0.33	10
accuracy			0.80	40
macro avg	0.89	0.60	0.61	40
weighted avg	0.84	0.80	0.75	40

Source : (Research Results, 2025)
Figure 6. Result Test

The model achieved an overall test accuracy of 80.00%, indicating that it correctly classified 80% of the test images. However, a closer analysis of class-wise metrics reveals a significant performance gap between the negative and positive classes:

1. Negative Class: Precision = 0.79, Recall = 1.00, F1-score = 0.88
2. Positive Class: Precision = 1.00, Recall = 0.20, F1-score = 0.33

These results indicate that the model performs exceptionally well at identifying negative cases (100% recall) but struggles to detect positive cases (only 20% recall). Although every positive prediction made by the model was correct (precision = 100%), many actual positive cases were misclassified as negative, suggesting a bias toward the majority class The macro-average F1-score was 0.61, while the weighted-average F1-score was 0.75, further reflecting the imbalance in model performance between classes. The high precision but low recall for the positive class indicates that the model is conservative in predicting positives, possibly due to class imbalance in the dataset Figure 6 illustrates the classification results, visually confirming the model's tendency to correctly identify most negative samples while frequently failing to recognize positive samples.

Interpretation and Implications

While the overall accuracy appears reasonably high, the low recall for the positive class is concerning in the context of cervical cancer detection, where false negatives could have severe implications for patient outcomes. In medical diagnostics, high sensitivity (recall) for positive cases is crucial to ensure that all potential cases are flagged for further examination.

To address this limitation, several strategies could be considered:

1. Data Balancing: Oversampling positive cases or undersampling negative cases to reduce class imbalance.
2. Threshold Tuning: Adjusting the decision threshold to favor higher recall for the positive class.
3. Hybrid Model Integration: Combining VGG16 with other classifiers or attention-based mechanisms to improve sensitivity.
4. Advanced Data Augmentation: Introducing more synthetic variations of positive cases to improve the model's exposure to positive patterns.

implementing these strategies, the model's ability to detect positive cervical cancer cases could be significantly improved, making it more suitable for clinical decision support systems.

CONCLUSION

This study successfully developed and optimized the VGG16 architecture for Pap smear image classification in cervical cancer detection by leveraging transfer learning and data augmentation techniques. The training results demonstrated a significant improvement in training accuracy, reaching 98.50%, although validation accuracy remained stable at 88.24%, suggesting a potential

Accredited Rank 2 (Sinta 2) based on the Decree of the Dirjen Penguatan RisBang Kemenristekdikti No.225/E/KPT/2022, December 07, 2022. Published by LPPM Universitas Nusa Mandiri

VOL. 11. NO. 3 FEBRUARI 2026
P-ISSN: 2685-8223 | E-ISSN: 2527-4864
DOI: 10.33480/jitk.v11i3.7131

risk of overfitting. Evaluation on the unseen test dataset achieved an overall accuracy of 80.00%, with excellent performance for the negative class but considerably lower recall for the positive class. This indicates that the model tends to be biased toward the majority (negative) class, which could lead to missed detections of positive cervical cancer cases. The findings highlight the necessity of implementing additional strategies to improve model sensitivity toward positive cases, such as data balancing, decision threshold adjustment, and hybrid model integration. The key contribution of this research lies in adapting and optimizing the VGG16 architecture specifically for Pap smear image characteristics, which can serve as a foundation for developing reliable clinical decision support systems for early cervical cancer screening. Future research is recommended to expand the dataset, apply more advanced data balancing techniques, and explore the integration of VGG16 with other deep learning architectures to enhance generalization performance and diagnostic accuracy.

ACKNOWLEDGEMENTS

The authors would like to express their deepest gratitude to the Ministry of Higher Education, Science, and Technology of the Republic of Indonesia, through the Directorate General of Research and Development, for the funding and support provided through the Beginner Lecturer Research Grant (Hibah Penelitian Dosen Pemula) 2025, which made this study possible. Special thanks are also extended to STMIK IKMI Cirebon for the continuous support, assistance, and facilities provided throughout the research process. The authors sincerely acknowledge the collaboration of Sumber Waras Hospital, Cirebon, for providing valuable cooperation in this study. Furthermore, the authors wish to thank the International Agency for Research on Cancer (IARC) for their contribution and the provision of essential reference data, which were instrumental in supporting the successful completion of this research.

REFERENCE

[1] M. Kalbhor, S. Shinde, P. Wajire, and H. Jude, "CerviCell-detector: An object detection approach for identifying the cancerous cells in pap smear images of cervical cancer," *Heliyon*, vol. 9, no. 11, 2023, doi: 10.1016/j.heliyon.2023.e22324.

[2] R. Kundu and S. Chattopadhyay, "Deep features selection through genetic algorithm for cervical pre-cancerous cell classification," vol. 82, no. 9, pp. 13431–13452, 2023, doi: 10.1007/s11042-022-13736-9.

[3] X. Zhang *et al.*, "FD-Net: Feature Distillation Network for Oral Squamous Cell Carcinoma Lymph Node Segmentation in Hyperspectral Imagery," vol. 28, no. 3, pp. 1552–1563, 2024, doi: 10.1109/JBHI.2024.3350245.

[4] B. Chitra, S. S. Kumar, and D. Subbulekshmi, "Prediction Models Applying Convolutional Neural Network based Deep Learning to Cervical Cancer Outcomes," vol. 70, no. 8, pp. 7058–7068, 2024, doi: 10.1080/03772063.2024.2305831.

[5] R. Ahmed, N. Dahmani, G. Dahy, A. Darwish, and A. E. Hassanien, "Early Detection and Categorization of Cervical Cancer Cells Using Smoothing Cross Entropy-Based Multi-Deep Transfer Learning," vol. 12, pp. 157838–157853, 2024, doi: 10.1109/ACCESS.2024.3485888.

[6] W. Gao, D. Wang, and Y. Huang, "Designing a Deep Learning-Driven Resource-Efficient Diagnostic System for Metastatic Breast Cancer: Reducing Long Delays of Clinical Diagnosis and Improving Patient Survival in Developing Countries," *Cancer Inform*, vol. 22, 2023, doi: 10.1177/11769351231214446.

[7] J. Yi, X. Liu, S. Cheng, L. Chen, and S. Zeng, "Multi-scale window transformer for cervical cytopathology image recognition," vol. 24, pp. 314–321, 2024, doi: 10.1016/j.csbj.2024.04.028.

[8] M. Salehi, A. Vafaei Sadr, S. R. Mahdavi, H. Arabi, I. Shiri, and R. Reiazi, "Deep Learning-based Non-rigid Image Registration for High-dose Rate Brachytherapy in Inter-fraction Cervical Cancer," vol. 36, no. 2, pp. 574–587, 2023, doi: 10.1007/s10278-022-00732-6.

[9] Y. Khalifa, C. Donohue, J. L. Coyle, and E. Sejdić, "Autonomous Swallow Segment Extraction Using Deep Learning in Neck-Sensor Vibratory Signals From Patients With Dysphagia," vol. 27, no. 2, pp. 956–967, 2023, doi: 10.1109/JBHI.2022.3224323.

[10] J. B. A. Teixeira *et al.*, "Segmentation of cervical nuclei using convolutional neural network for conventional cytology," vol. 11, no. 5, pp. 1876–1888, 2023, doi: 10.1080/21681163.2023.2197086.

[11] R. Klangbunrueang, P. Pookduang, W. Chansanam, and T. Lunrasri, "AI-Powered Lung Cancer Detection: Assessing VGG16 and CNN Architectures for CT Scan Image

Classification," *Informatics*, vol. 12, no. 1, p. 18, 2025, doi: 10.3390/informatics12010018.

[12] V. Lakide, "Advancement of Lung Cancer Diagnosis With Transfer Learning: Insights From VGG16 Implementation," *Journal of Electronics Electromedical Engineering and Medical Informatics*, vol. 7, no. 3, pp. 729–739, 2025, doi: 10.35882/jeeemi.v7i3.704.

[13] Z. Hameed, S. Zahia, B. García-Zapirain, J. J. Aguirre, and A. M. Vanegas, "Breast Cancer Histopathology Image Classification Using an Ensemble of Deep Learning Models," *Sensors*, vol. 20, no. 16, p. 4373, 2020, doi: 10.3390/s20164373.

[14] F. Hashem *et al.*, "Exploring Data Imbalance Challenges in Cervical Cancer Detection Using Advanced Deep Learning Models," in *2024 IEEE International Conference on Smart Systems and Power Management, IC2SPM 2024*, 2024, pp. 95–101. doi: 10.1109/IC2SPM62723.2024.10841356.

[15] F. Hashem *et al.*, "Exploring Data Imbalance Challenges in Cervical Cancer Detection Using Advanced Deep Learning Models," in *2024 IEEE International Conference on Smart Systems and Power Management, IC2SPM 2024*, Institute of Electrical and Electronics Engineers Inc., 2024, pp. 95–101. doi: 10.1109/IC2SPM62723.2024.10841356.

[16] L. W. Habtemariam, E. T. Zewde, and G. L. Simegn, "Cervix Type and Cervical Cancer Classification System Using Deep Learning Techniques," *Medical Devices Evidence and Research*, vol. Volume 15, pp. 163–176, 2022, doi: 10.2147/mder.s366303.

[17] H. Yi, "A Review of Convolutional Neural Networks in Cancer Image Classification," *Applied and Computational Engineering*, vol. 97, no. 1, pp. 69–74, 2024, doi: 10.54254/2755-2721/97/20241334.

[18] R. Maurya, N. Nath Pandey, and M. Kishore Dutta, "VisionCervix: Papanicolaou cervical smears classification using novel CNN-Vision ensemble approach," *Biomed Signal Process Control*, vol. 79, 2023, doi: 10.1016/j.bspc.2022.104156.

[19] P. Yadav, A. Gupta, A. Parveen, and A. Kumar, "Advancement in Deep Learning Methods for Diagnosis and Prognosis Of Cervical Cancer," *Curr Genomics*, vol. 23, no. 4, pp. 234–245, 2022, doi: 10.2174/1389202923666220511155939.

[20] M. Arya, P. K. Yadav, A. Jain, M. Gupta, S. Agarwal, and A. S. Rajpoot, "Neural Network to detect Cervical Cancer early using Pap smears Images," in *Proceedings of International Conference on Contemporary Computing and Informatics, IC3I 2024*, 2024, pp. 324–329. doi: 10.1109/IC3I61595.2024.10828866.

[21] W. Huang, S. Sun, Z. Yu, S. Lu, and H. Feng, "Chronic Cervicitis and Cervical Cancer Detection Based on Deep Learning of Colposcopy Images Toward Translational Pharmacology," *Front Pharmacol*, vol. 13, 2022, doi: 10.3389/fphar.2022.911962.

[22] T. Yang, H. Hu, X. Li, M. Qing, L. Chen, and Q. Huang, "A pyramid convolutional mixer for cervical pap-smear image classification tasks," *Biomed Signal Process Control*, vol. 99, 2025, doi: 10.1016/j.bspc.2024.106789.

[23] O. Attallah, "CerCan·Net: Cervical cancer classification model via multi-layer feature ensembles of lightweight CNNs and transfer learning," vol. 229, 2023, doi: 10.1016/j.eswa.2023.120624.

[24] S. Jung, S. Wang, and D. Lee, "CancerGATE: Prediction of cancer-driver genes using graph attention autoencoders," vol. 176, 2024, doi: 10.1016/j.compbiomed.2024.108568.

[25] L. Mishra, R. Dasgupta, Y. S. Chowdhury, S. Nanda, and S. Nanda, "Cervical Cancer Detection Using Hybrid Pooling-Based Convolutional Neural Network Approach," *Indian J Gynecol Oncol*, vol. 21, no. 2, 2023, doi: 10.1007/s40944-023-00712-w.

[26] C. Zhang, D. Jia, Z. Li, and N. Wu, "Auxiliary classification of cervical cells based on multi-domain hybrid deep learning framework," *Biomed Signal Process Control*, vol. 77, 2022, doi: 10.1016/j.bspc.2022.103739.

[27] A. Khan, S. Han, N. Ilyas, Y.-M. Lee, and B. Lee, "CervixFormer: A Multi-scale swin transformer-Based cervical pap-Smear WSI classification framework," vol. 240, 2023, doi: 10.1016/j.cmpb.2023.107718.

Accredited Rank 2 (Sinta 2) based on the Decree of the Dirjen Penguatan RisBang Kemenristekdikti No.225/E/KPT/2022, December 07, 2022. Published by LPPM Universitas Nusa Mandiri